NANO LETTERS

Letter

pubs.acs.org/NanoLett

DNA-Linker-Induced Surface Assembly of Ultra Dense Parallel Single Walled Carbon Nanotube Arrays

Si-ping Han,[†] Hareem T. Maune,[§] Robert D. Barish,[∥] Marc Bockrath,[‡] and William A. Goddard, III*[,†,⊥]

[†]Materials and Process Simulation Center, California Institute of Technology, Pasadena California 91125, United States

[‡]Department of Physics, University of California, Riverside, California 92521, United States

[§]IBM Almaden Research Center, San Jose, California 95120, United States

[∥]Wyss Institute, Harvard University, Cambridge, Massachusetts 02138, United States

[⊥]Graduate School of EEWS (WCU), Korea Advanced Inst. Science Technology, Daejeon, Republic of Korea

Supporting Information

ABSTRACT: Ultrathin film preparations of single-walled carbon nanotube (SWNT) allow economical utilization of nanotube properties in electronics applications. Recent advances have enabled production of micrometer scale SWNT transistors and sensors but scaling these devices down to the nanoscale, and improving the coupling of SWNTs to other nanoscale components, may require techniques that can generate a greater degree of nanoscale geometric order than has thus far been achieved. Here, we introduce linker-induced surface assembly, a new technique that uses small structured DNA linkers to assemble solution dispersed nanotubes into parallel arrays on charged surfaces. Parts of our linkers act as spacers to precisely control the internanotube separation distance down to <3 nm and can serve as scaffolds to position components such as proteins between adjacent parallel nanotubes. The resulting arrays can then be stamped onto other substrates. Our results demonstrate a new paradigm for the self-assembly of anisotropic colloidal nanomaterials into ordered structures and provide a potentially simple, low cost, and scalable route for preparation of exquisitely structured parallel SWNT films with applications in high-performance nanoscale switches, sensors, and meta-materials.

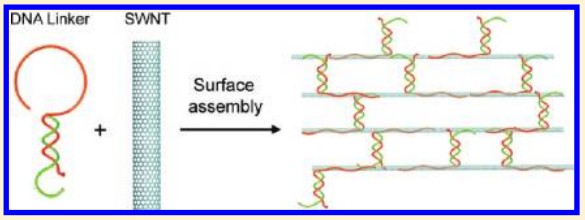

KEYWORDS: *self-assembly, DNA nanotechnology, carbon nanotubes, colloidal nanomaterials*

The self-assembly of solution dispersed single-walled carbon nanotubes (SWNT)[1] and other geometrically anisotropic colloidal nanomaterials[2,3] into ordered arrays[4,5] requires alignment and orientation of irregularly shaped nanoscale objects along multiple axes to achieve particular desired arrangements. Satisfactory general solutions could enable scalable and economical continuous manufacturing processes that use liquid phase handling[1,6] to take bulk synthesized nanomaterials through multiple stages of chemical modification[7] and purification[8,9] before incorporation into real products as high performance nanostructured elements.[5,6,10]

An important example of anisotropic nanoassembly is the arrangement of nanowires[11] and carbon nanotubes[5] into monolayer parallel arrays, which can maximize packing density without compromising each wire's electrical isolation and accessibility, thus enabling defect tolerant nanofabrics[12−14] and other technologies with transformative logic, memory, interface, and sensor applications.[15−17] Existing top down methods can create parallel arrays from solution-dispersed nanowires or SWNTs by applying alignment forces during deposition or film formation,[18−21] or by creating chemically patterned deposition substrates,[22,23] but array densities greater than 30 μm^{-1} (vs ~1000 μm^{-1} maximum possible density for SWNTs) have not been achieved, and control over wire spacing at sub 100 nm scales have proven elusive. Alternatively, we previously attached SWNTs to self-assembled DNA origami templates that can have sub-10 nm feature resolution,[24] but this increases complexity and cost; the ordered structure cannot be larger than the limited size of the DNA nanostructure and the chemical and geometric details of wire-template attachment introduces 10 nm scale uncertainties in wire spacing. Thus, both top down and bottom up methods have notable shortcomings.

Our new linker-induced surface assembly (LISA) process combines top down and bottom up forces to assemble ultradense parallel SWNT arrays. In the LISA process, pristine SWNTs are sonicated in an aqueous salt solution with multidomain DNA linkers (Figure 1a) that cooperatively disperse each nanotube via noncovalent wrapping of single stranded DNA[1,25] around the nanotube sidewall. The resulting colloid (Figure 1b) can remain stable for weeks under ambient conditions, but the DNA-SWNTs will deposit onto charged substrates in the presence of divalent counterions, which form salt bridges[26] between nanotube-anchored DNA linkers and

Received: May 29, 2011
Revised: January 24, 2012
Published: February 9, 2012

   dx.doi.org/10.1021/nl201818u | *Nano Lett.* 2012, 12, 1129−1135

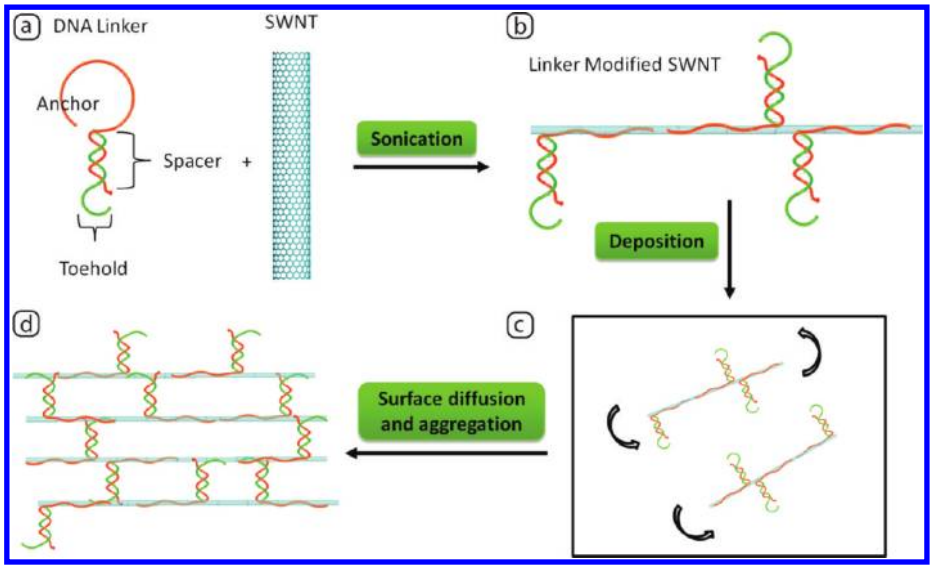

Figure 1. The assembly process. (a) Structured DNA linkers are combined with unmodified SWNTs and sonicated to produce (b) SWNTs with noncovalently anchored DNA linkers. (c) Upon deposition, the nanotubes can diffuse along the surface and assemble into (d) parallel arrays. The DNA duplex in each linker positions itself between the adjacent SWNTs as a rigid spacer.

surface charge groups. When monovalent counterions are then introduced to the deposition droplet, the DNA-SWNTs diffuse in 2D along the deposition surface (Figure 1c) (likely due to disruption of salt bridge interactions[26]). Under surface confinement, weak dispersive interactions between DNA linkers on one nanotube and the sidewall of neighboring nanotubes can cooperatively induce assembly of parallel SWNTs arrays. The double-stranded domains of the DNA linkers then sit between the adjacent nanotubes to keep them at a fixed distance, resulting in arrays with uniform pitch (Figure 1d).

We first discovered the self-assembly process when examining SWNTs dispersed using DNA oligonucleotide linkers possessing both single-stranded and double-stranded domains (Figure 1a). Deposition of nanotubes bearing 20 base pair DNA duplexes on Muscovite mica at near monolayer surface coverage under 1xTAE Mg buffer (10 mM tris acetate, 1 mM EDTA, 12.5 mM magnesium acetate in water) resulted in formation of a large number of dimers and trimers of parallel SWNTs. The internanotube separation appeared to be uniform (~ 7 to 9 nm from center to center). When the process was repeated at lower surface concentration of SWNTs or in the presence of 1 mM Ni acetate (known to inhibit DNA duplex mobility on the mica surface[26]), there were far fewer assembled nanotubes. Since we had observed that DNA dispersed SWNTs under 1xTAE Mg buffer can move on the mica surface as they are imaged by tapping mode atomic force microscopy (AFM), we hypothesized that the dimers and trimers might be forming via association of neighboring SWNTs on the deposition substrate.

To test the surface assembly hypothesis, we experimented with a procedure aimed at encouraging surface diffusion. Past studies[2] and our experiences have shown that DNA nanostructures adhering to mica under Mg^{2+} solutions can exhibit substantial surface diffusion in the presence of a high concentration of Na+, which disrupts mica-Mg^{2+} -DNA salt bridges. To utilize this effect, we first deposited the DNA-SWNTs using 1xTAE Mg buffer, and then we replaced the solution covering the substrate with phosphate buffered NaCl at 0.75−2 M concentrations. Tapping mode AFM images of deposited SWNTs under these conditions revealed substantial surface movement, while larger multinanotube assemblies appeared to have substantially lower surface mobility than individual SWNTs (Supporting Information Figure S1). When mica substrates with SWNTs incubated under NaCl were washed in 1xTAE Mg buffer and imaged with the addition of 1 mM Ni Acetate (known to inhibit DNA surface movement), we found that the majority of nanotubes had assembled into structures composed of two or more parallel SWNTs (Supporting Information Figure S2). This occurred regardless of nanotube concentration on the mica surface or the presence or absence of perturbation by tapping mode AFM. Interestingly, varying the NaCl concentration and the surface density of deposited SWNTs seemed to have little effect on the width of the SWNT arrays (2 to 6 SWNTs on mica). We suspect that the nonlinear drop in surface mobility observed for multinanotube arrays may be a self-limiting mechanism for the array size. Taken together, these observations strongly suggest that SWNTs assemble due to surface diffusion.

In addition to Muscovite mica, we also experimented with array assembly on substrate-supported *Dipalmitoylphosphatidylcholine* (DPPC) lipid bilayers.[27] These bilayers can form on a variety of substrates, are compatible with lithographic patterning, and are frequently used to model biological membranes. At room temperature, DPPC bilayers are in the solid phase (T_m = 41 °C) with a smooth surface composed of densely packed polar headgroups that allow counterion mediated surface diffusion of DNA modified SWNTs. The adhesion of DNA-SWNTs to the bilayer surface seems very sensitive to NaCl concentration. In the presence of 1xTAE Mg, all SWNTs desorbed from the surface when the solution concentration of NaCl exceeded 0.45 M. This suggests that even relatively large SWNT arrays may have some degree of surface mobility on DPPC at ~0.45 M NaCl concentrations. This makes it easier to control array diffusion and assemble wider arrays, and we were able to produce parallel SWNT arrays up to 11 nanotubes wide by incubating SWNTs under 1xTAE Mg + 0.35 M NaCl buffer at room temperature (Supporting Information Figure S3).

dx.doi.org/10.1021/nl201818u | *Nano Lett.* 2012, 12, 1129−1135

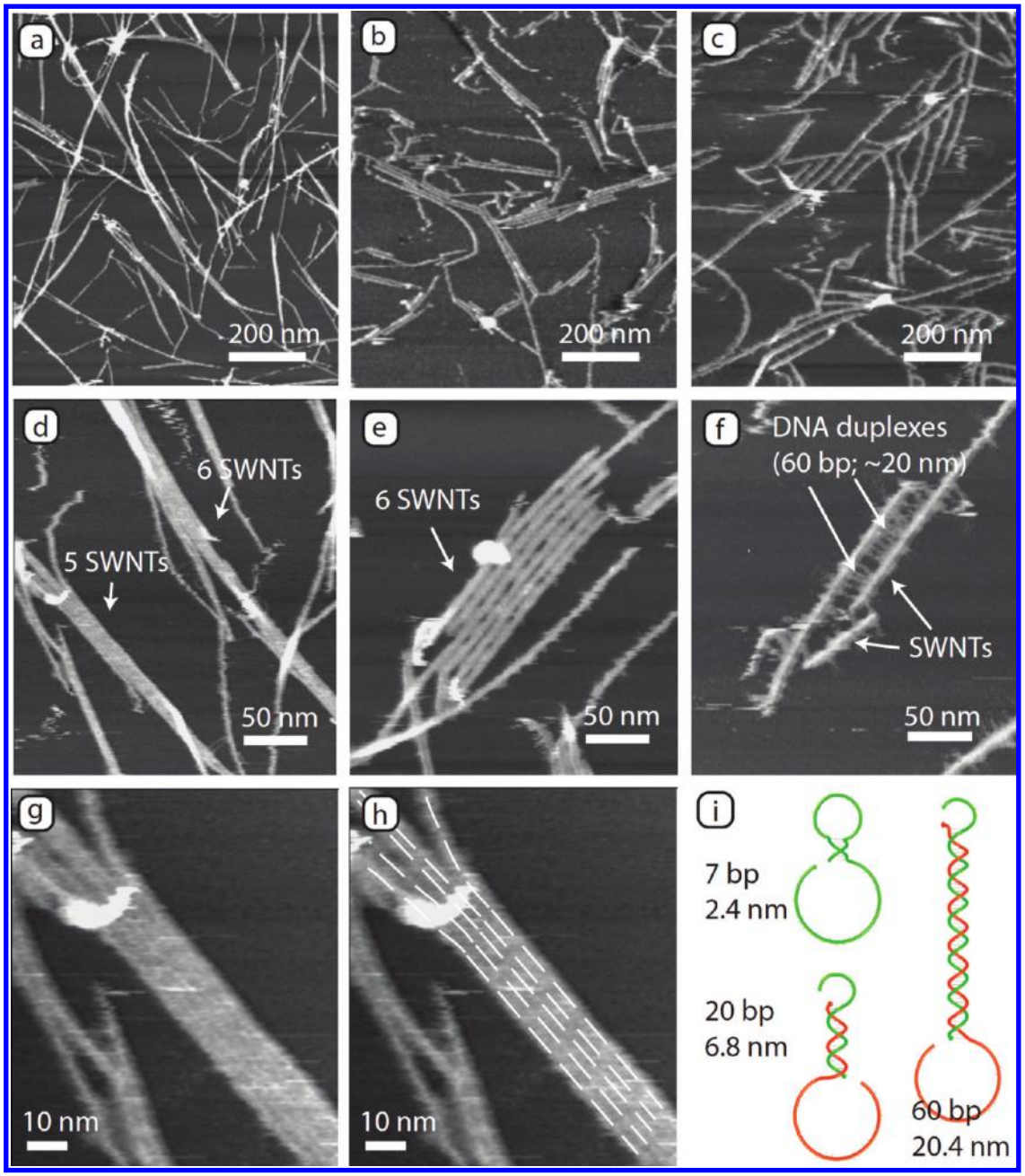

Figure 2. Tapping mode AFM showing topography of SWNT arrays on mica under fluid. (a,d,g,h) Arrays formed with 7 bp DNA spacers. (g,h) The 5 SWNT array from panel d with the dashed lines in panel h representing the approximate positions of the SWNTs. The measured array pitch was determined to be less than 3 nm. SWNT arrays with 20 bp (b,e) and 60 bp spacers (c,f) have array pitch of ~8.5 and ~22 nm, respectively. (i) The structure of DNA linkers with 7, 20, and 60 bp. Notice that the linker with the 7 bp spacer is a hairpin while the larger linkers are constructed from 2 strands.

Since DNA-modified SWNTs adhere to the negatively charged mica and polar DPPC surfaces via relatively weak Mg^{2+} mediated electrostatic interactions, we reasoned that a surface with densely packed positive charges might adhere more strongly to the DNA phosphate backbone groups and out-compete mica and DPPC for retention of assembled arrays. Thus, we clamped (Supporting Information Figure S4) mica and DPPC substrates carrying assembled SWNT arrays onto γ-amino propyl silane functionalized glass slides (Corning Life Sciences), which had a high surface density of positively charged primary amine groups. To facilitate the transfer, we first added NaCl to the assembly substrates to weaken binding of DNA-SWNTs with the mica surface. After ~2.5 h, the clamped surfaces were carefully peeled apart. AFM scans showed that a large number of SWNT arrays transferred onto the glass surface while maintaining their parallel structure and uniform pitch of ~8.3 nm. While stamping from the DPPC surface resulted in transfer of some DPPC patches along with the nanotubes, transfer from mica was relatively clean (Supporting Information Figure S5). This demonstrates a simple method for transferring assembled arrays onto silica based substrates suitable for lithographic device fabrication.

Supporting Information Figure S6 shows a high-resolution AFM scan of a SWNT dimer assembled using DNA linkers that

dx.doi.org/10.1021/nl201818u | *Nano Lett.* 2012, 12, 1129–1135

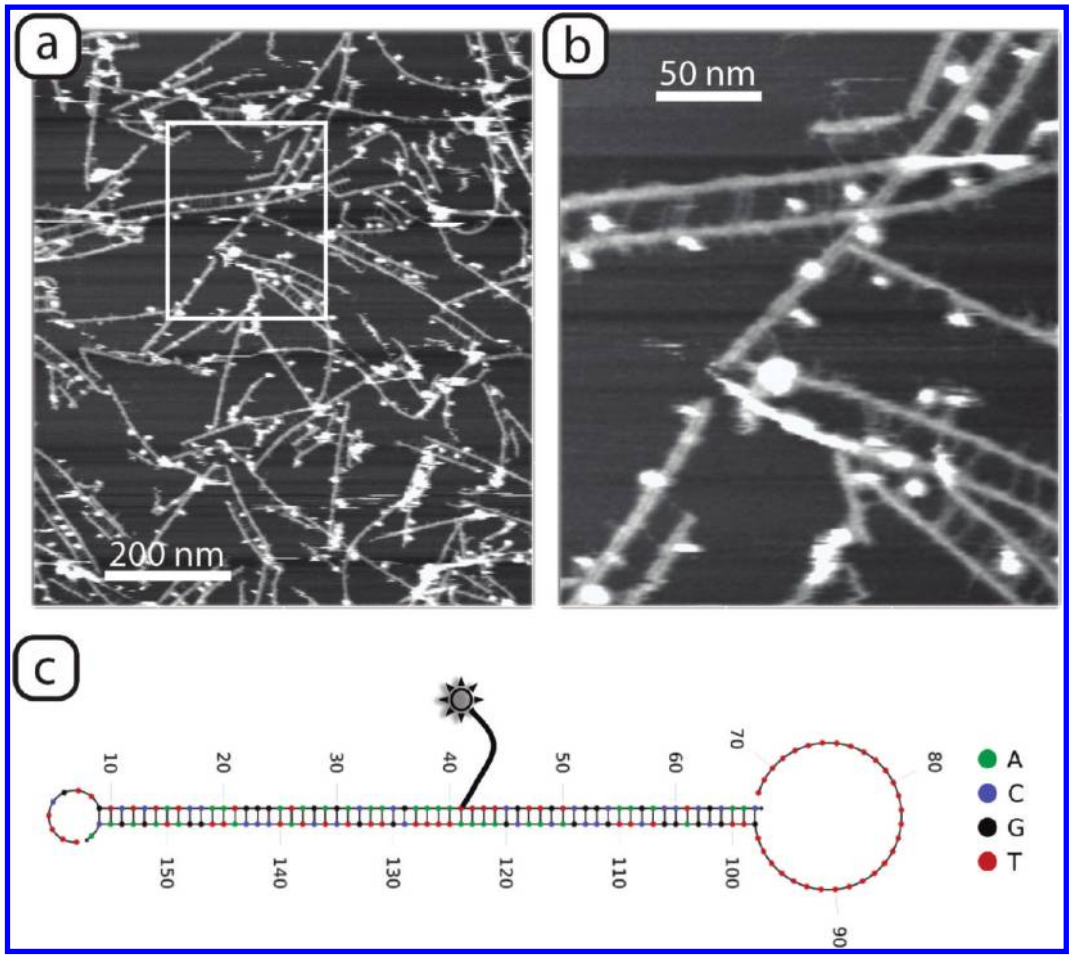

Figure 3. Tapping mode AFM of SWNT arrays with biotin-modified 60 bp spacers and attached Streptavidin proteins on mica under salt buffer solution. The boxed area in panel a is magnified in panel b. Streptavidin proteins (bright spots) are seen on DNA duplexes bridging adjacent SWNTs. Note that some Streptavidin proteins are attached to DNA duplexes that are pointing away from the adjacent SWNT. (c) The position of the biotin linker on the modified DNA linker.

possessed 20 bp spacer domains. This scan revealed a ladderlike structure with dense "rungs" connecting adjacent parallel SWNTs. From our previous work,[24] we knew that the 30 nucleotide (nt) long polythymine dispersal domains of our linkers likely adsorbed strongly onto the SWNT surface. We also knew that our duplex spacer and short toehold domains (Figure 1a) likely remained free from the nanotube surface (Figure 1b). Of the two, the duplex is the only one large enough (6.8 nm) to appear as the ladder rungs in Supporting Information Figure S6. Thus, we suspected that the DNA duplexes were situated between the SWNTs as rigid spacers while the toeholds adsorbed weakly onto accessible sidewall surfaces on the adjacent nanotube. Together, the rigid separators and sticky ends of numerous DNA linkers along each DNA-SWNT can cooperatively induce the assembly and alignment of diffusing SWNTs and keep them at a uniform internanotube separation. If true, then the array pitch should closely correlate with the length of the DNA duplexes.

To test the above hypothesis, we created DNA linkers with 7 bp (2.38 nm), 20 bp (6.8 nm, and 60 bp (20.4 nm) long duplex domains and used them to assemble arrays of CoMoCat SWNTs[28] (Southwest Nanotechnologies Inc., Norman, OK) (Figure 2) (the linker with the 7 bp spacer was formed from a single hairpin DNA due to energetic stability considerations; see Methods and Materials for detailed explanation). Approximately 82% of nanotubes with 20 bp spacers and 52% of nanotubes with 60 bp spacers assembled into parallel arrays (Supporting Information Table S1). This resulted in the formation of arrays with ~2.9, ~8.5, and ~22 nm pitch, as measured by AFM. To our knowledge, the ~2.9 nm arrays (Figure 2a,d,g,h) represent the highest density packing of parallel SWNTs achieved to date (~345 SWNTs μm^{-1}).

Although the limitations of our AFM prevented consistent resolution of 7 bp and 20 bp spacers, the 60 bp spacers were clearly imaged (Figure 2f). Most spacers between adjacent SWNTs spanned the gap from one nanotube to the next, thus giving strong evidence for the hypothetical structure depicted in Figure 1d. Interestingly, most of the 60 bp spacers appear to be oriented nearly perpendicular to the axis of their nanotubes. To better understand the interaction of our DNA linkers with the SWNT sidewall, we attempted array assembly for HiPco[29] P2 SWNTs (Carbon Solutions Inc., Riverside, CA) using a series of linkers possessing 30 nt anchor, 20 bp spacer, and 0, 5, 7, 9, or 11 nt toehold domains. Using identical procedures, we also attempted to array assembly using P2 SWNTs dispersed with single-stranded DNA. As expected, SWNTs dispersed using single-stranded DNA did not assemble into parallel arrays. For linkers with spacer domains, all toehold lengths resulted in array assembly. The portion of nantoubes that assembled into arrays increased with toehold length (Supporting Information

dx.doi.org/10.1021/nl201818u | *Nano Lett.* 2012, 12, 1129–1135

Table 1. Sequences of DNA Strands

strand	sequence	special instructions
7 bp hairpin linker	5′-GCCGGGCTTTTTTTTTTTTTTTTGCCCGGCTTTTTTTTTTT TTTTTTTTTTTTTTTTTT-3′	standard desalting
20 bp anchor side	5′-TTTTTTTTTTTTTTTTTTTTTTTTTTTTTTGTTGCGAGGTCT TGCCGACA-3′	standard desalting
20 bp toehold side:		
0 base toehold	5′-TGTCGGCAAGACCTCGCAAC-3′	standard desalting
5 base toehold	5′-TTCGTTGTCGGCAAGACCTCGCAAC-3′	standard desalting
7 base toehold	5-TTTTCGTTGTCGGCAAGACCTCGCAAC-3	standard desalting
9 base toehold	5′-TTTTTTCGTTGTCGGCAAGACCTCGCAAC-3′	standard desalting
11 base toehold	5′-TTTTTTTTCGTTGTCGGCAAGACCTCGCAAC-3′	standard desalting
60 bp anchor side	5′-TTTTTTTTTTTTTTTTTTTTTTTTTTTTTTGTTGCGAGGTCT TGCCGACAACGAAAATTTTCGTTGTCTCTATCCCATTGGATAGAGACA-3′	ultramer, no purifiaction
60 bp toehold side; no biotin	5′-TTTTCGTTGTCTCTATCCAATGGGATAGAGACAACGAA AATTTTCGTTGTCGGCAAGACCTCGCAAC-3′	ultramer, no purifiaction
60 bp toehold side; internal biotin	5′-TTTTCGTTGTCTCTATCCAATGGGATAGAGACAACGAAAA/iBiodT/ TTTCGTTGTCGGCAAGACCTCGCAAC-3′	page purified

Table S1), and the highest assembly efficiency of 67% was achieved using 11 nucleotide long toeholds. However, SWNTs dispersed with 11 base long toeholds were also more prone to aggregation while in solution.

Surprisingly, DNA linkers without toeholds were also able to induce formation of parallel arrays. We believe that three types of sticky end interactions may have contributed to SWNT assembly. First, we did not purify the synthesized oligonucleotides. Thus, linkers composed of truncated DNA strands would have been present in solution, and some of these may have had dangling single-stranded DNA on the end of the spacer domain. Second, the terminal A-T base-pair on the duplex spacer is unstable at room temperature. Thus, one or more base pairs may be able to dissociate and adsorbed onto the sidewall of the SWNT. Finally, DNA duplex blunt ends may have favorable dispersive interactions with the SWNT sidewall. This may also contribute to the nearly perpendicular orientation of DNA spacers relative to the axis of assembled nanotubes.

With the structures of the arrays known, an unresolved question is why DNA-SWNTs can remain dispersed in solution but assemble after deposition. We do not yet understand the detailed causes. However, as our experience with the 11 nt toehold linkers demonstrates, a likely significant factor is the weakness of individual toehold−nanotube interactions and the resulting requirement for cooperation between linkers to induce nanotube assembly. On the deposition substrate, the confinement of DNA linkers to the plane of the substrate may then favor the cooperative toehold-sidewall sticky interactions necessary for assembly.

DNA spacers in the assembled arrays offer convenient scaffolds for arrangement of heterogeneous molecular, macromolecular, and nanoscale components between parallel SWNTs. To demonstrate this we modified the 60 bp spacer by changing one of its internal dTs to a biotin linked dT. The position of this modification (35th base-pair from the base of the toehold) puts it ∼12 nm from the toehold side and ∼8.5 nm from the anchor. We found that SWNTs with the biotinylated linker assembled on mica without issue. When Streptavidin was added to assembled arrays (∼18 nM concentration), they attached to DNA spacers at the designated positions between adjacent SWNTs (Figure 3).

Conclusion. LISA opens a new route for using DNA-dispersed SWNTs to produce parallel SWNT arrays with diverse applications. Unlike other methods,[2,4,30,31] surface diffusion plays a central role in the LISA process. This has two advantages. First, as is the case with SWNTs (flexible one-dimensional rods with extreme length to width ratio), surface confinement can limit the orientation and conformational freedom of anisotropic nanomaterials and their conjugated linkers to allow rapid assembly of arrays not easily obtainable in three dimensions. Second, it may be possible to corral surface diffusion using top-down alignment forces[5,6,20] or micro or nanoscale surface patterning,[22,23,32] and this may allow control over array alignment, placement, and size.

A key enabler of the LISA method is the use of structured DNA linkers. Although single-stranded DNA has long been used in colloidal nanoassembly,[33,34] only recently have we[24] and others[35] begun utilizing rational design of secondary and tertiary structure to control the kinetics of the assembly process and the geometry of the resulting structures. In the present study, the duplex spacer and single-stranded toehold domains influence solution phase aggregation and surface diffusion, drive surface assembly, determine array geometry, and provide scaffolding for additional modifications. It may be possible to develop LISA-like assembly processes for other anisotropic nanomaterials by designing conformational mismatches and entropic barriers that can be alleviated by surface confinement. Indeed, surface-mediated assembly has recent been achieved for pure DNA nanostructures.[36]

Parallel SWNT arrays with sub-20 nm uniform spacing present new opportunities in basic and applied nanoscience. Uniformly metallic or semiconducting SWNTs[8,37] arrays may substantially improve the performance of SWNT based nanoelectronics.[38] Further improvements in the assembly technique could allow the implementation of nanofabric type architectures[12,16,39] at densities approaching 1 device every 10 nm^2. The use of ultradense SWNT arrays to create electronic or optical metamaterials should also be considered. Indeed theoretical calculations have shown[40] that the application of superlattice electrical potentials with 10 nm scale periodicities to graphene could lead to supercollimation of electrons propagating in graphene in the direction of the periodicity, and experimental measurements have shown SWNTs to be ideal excitonic optical wires that can exhibit optical coupling when arranged in parallel.[39] Finally, the macromolecular scale is the operating scale of biological machinery. Recent developments[41−44] suggest an emerging convergence of nanoelectronics and single molecule biophysics. SWNTs have advantageous geometric and chemical properties for applications in bioelectronics.[42,43,45,46] Arrays assembled with LISA can have nanotube spacing adjusted to match the size of biomolecular components and their integral DNA spacers can scaffold

biomolecule placement. We believe that this may enable the assembly of new bioelectronic (Supporting Information Figure S7) or nanofluidic (Supporting Information Figure S8) interfaces for sensing or processing biomolecules.

- **Methods and Materials.** *Materials.* CoMoCat single-walled carbon nanotubes were purchased from Southwest Nanotechnologies (Norman, OK) in powder form and used as received. Alternatively, P2 SWNTs can be purchased from Carbon Solutions (Riverside, CA).
- Custom DNA was ordered from Integrated DNA Technologies (Coralville, Iowa), dissolved in Milli-Q water and kept frozen at −20 °C. Sequences are listed in Table 1.
- Dipalmitoylphosphatidylcholine (DPPC) was obtained in powder form from Avanti Polar Lipids (Alabaster, Alabama).
- GAPS II microarray slides were obtained from Corning Life Sciences (Lowell, Ma).

Formation of DNA Linkers. DNA linker strands are added to ∼33 μM concentration in 500 μL of 1xTAE Mg buffer (10 mM tris acetate, 1 mM EDTA, 12.5 mM magnesium acetate). When two strands are used for the linker, the toehold side strand is added at 10% excess to the anchor side.

The linker solution is then partitioned into 100 μL aliquots and annealed in a PCR thermal cycler (95 °C for 1 min, then cool to 20 at 1 °C per minute).

Dispersal of SWNTs. The annealed linkers are added to ∼0.5−1 mg of SWNTs in a 1.6 mL PCR tube. This solution is then sonicated for ∼60 min in a Branson 2510 bath sonicator until the SWNTs are dispersed. For this operation the water level in the sonicator can be reduced from the standard operating level to increase applied power.

Following sonication, the SWNT linker solution is centrifuged at 16 000 g at 4 °C for 90 min. The supernatant is recovered and the retenate is discarded.

The dispersed SWNT solution can remain stable at 4 °C for up to 1 month. The 100 μL aliquots can be stored indefinitely at −80 °C.

Assembly of CoMoCat SWNTs on Mica. A sample of 2.5−20 μL of dispersed SWNTs were added to ∼4 cm^2 pieces of Muskovite mica, then 1xTAE Mg is added to bring the drop to 20 μL. After 5 min at room temperature, 80 μL of solution containing 1.5 M NaCl and 0.1 M Na_2HPO_4 is added to the existing droplet. (The exact concentration of NaCl does not seem to significantly affect the assembly process. NaCl (0.5 to >2 M) with either no buffer, or 1xTAE, or 0.01 to 0.1 M Na_2HPO_4 will all work).

Assembly is not very sensitive to incubation conditions. Best results were achieved for 30 min incubations at 40 °C. But room temperature incubations from 15 min to 12 h will generally result in good assembly as long as measures are taken to prevent drying of the deposition droplet.

For stable imaging using fluid mode AFM, the buffer is first exchange to 1xTAE Mg by removing 50 μL from the droplet using a pipet, then adding 50 μL of 1xTAE Mg. This is repeated five times. Finally, 50 μL of the droplet is removed (leaving 50 μL), and a 10 μL drop of 10 mM Ni acetate is then added.

Assembly of HiPco SWNTs on Mica. HiPco P2 SWNTs were dispersed in 1xTAE Mg buffer as described above. For assembly, 5 μL of dispersed SWNTs were mixed in a vial with 45 μL of a solution with 1 M NaCl and (1/8)xTAE Mg. This was deposited on freshly cleaved mica for 1 h before replacement of the solution with the 1xTAE Mg and Ni acetate solution as described above.

Preparation on DPPC. DPPC was dissolved in 0.2 M NaCl and 0.01 M mono and di sodium phosphate buffer (∼pH 7.5) at 25 mg/mL concentration and ∼50 nm wide liposomes were formed via either extrusion or sonication using standard methods. The stock solution can be stored at 4 °C for 2 months. Immediately before formation of the bilayer, the stock solution is diluted to 2.5 mg/mL concentration in either 1xTAE mg buffer or in 2 mM $CaCl_2$, 0.2 M NaCl and 0.01 M mono and disodium phosphate.

For the substrate, glass coverslips or silicon wafers with native oxide are cleaned and cleaved into ∼4 cm^2 pieces. Immediately before deposition of lipids, the coverslips are treated to increase their hydrophilicity. (Thirty microliters of spectroscopy grade ethanol is added to each cut piece, ignited with a butane lighter, and allowed to burn. This can be repeated one or two times as needed.)

A sample size of 50 to 100 μL of 2.5 mg/mL DPPC is then added to the piece, which is then sealed in an airtight chamber and incubated in a PCR thermal cycler for 30 min at 50 °C. The temperature is then lowered to room temperature at a rate of 1 °C every 10 s. The glass or silicon substrate is then washed with 1xTAE Mg + 0.35 M NaCl buffer without exposing the surface to air (a good method is to remove 50 μL from the droplet with a pipet, add 50 μL of the washing solution, and repeat 5−10 times). Finally, 50 μL of 1xTAE Mg + 0.35 M NaCl buffer is left on the substrate.

Twenty microliters of dispersed SWNTs in 1xTAE Mg is added to the 50 μL droplet and the substrate carrying the SWNT solution is allowed to incubate at room temperature in a wet chamber for at least 2 h. The substrate is then imaged under 1xTAE Mg + 0.35 M NaCl buffer.

Addition of Streptavidin. For Streptavidin binding, substrates with well-formed SWNT arrays are washed and covered with 50 μL 1xTAE Mg. A 10 μL droplet of 200 nM Streptavidin in 1xTAE Mg is then added and the mixture is allowed to incubate at room temperature in a wet chamber for 1 h.

Stamping. For stamping the SWNTs formed on mica are covered with 1.5 M NaCl, 0.1 M Na_2HPO_4 buffer and clamped tightly to a piece of GAPS II microarray slide from Corning Life Sciences for 2 h.

For stamping the SWNTs formed on DPPC, well-formed SWNTs were covered in 1xTAE Mg + 0.35 M NaCl buffer and clamped to GAPS II microarray slides in a similar fashion. (See Supporting Information Figure S6.)

AFM Imaging. Images were collected by a Veeco (Plainview, NY) Nanoscope III system equipped with a fluid cell and a J scanner. The AFM was operated in tapping mode using Veeco SNL silicon nitride soft contact mode AFM tips (2 nm nominal tip radius, smaller cantilevers used). Amplitude set point was typically ∼0.4 V, drive amplitude ∼50 to 200 mV, integral gain of 0.3 to 0.5, frequency ∼10 kHz, and scan rate is typically 2 to 6 Hz.

■ ASSOCIATED CONTENT

Ⓢ Supporting Information

Additional information, figures, and tables. This material is available free of charge via the Internet at http://pubs.acs.org.

AUTHOR INFORMATION

Corresponding Author

*E-mail: wag@wag.caltech.edu.

Notes

We have filed provisional US patents on novel aspects of the work published here.

The authors declare no competing financial interest.

ACKNOWLEDGMENTS

We would like to thank Erik Winfree, Paul Rothemund, Sungwook Woo, Rizal Hariadi, and the other members of the DNA and Natural Algorithms Group at Caltech for generously sharing their facilities, resources, and insights. This work was initiated with support from an ONR Grant (N00014-09-1-0724) to MWB and from a grant to WAG from the Microelectronics Advanced Research Corporation (MARCO) and its Focus Center Research Program (FCRP) on Functional Engineered NanoArchitectonics (FENA). It was completed with funding from NSF-SNM (CMMI-1120890). WAG is also supported by the WCU (NRF R-31-2008-000-10055-0) program funded by the Korea Ministry of Education, Science and Technology.

REFERENCES

(1) Zheng, M.; Jagota, A.; Semke, E. D.; Diner, B. A.; McLean, R. S.; Lustig, S. R.; Richardson, R. E.; Tassi, N. G. *Nat. Mater.* **2003**, *2* (5), 338−342.

(2) Jones, M. R.; Macfarlane, R. J.; Lee, B.; Zhang, J.; Young, K. L.; Senesi, A. J.; Mirkin, C. A. *Nat. Mater.* **2010**, *9* (11), 913−917.

(3) Glotzer, S. C.; Solomon, M. J. *Nat. Mater.* **2007**, *6* (7), 557−562.

(4) Nykypanchuk, D.; Maye, M. M.; van der Lelie, D.; Gang, O. *Nature* **2008**, *451* (7178), 549−552.

(5) Cao, Q.; Rogers, J. A. *Adv. Mater.* **2009**, *21* (1), 29−53.

(6) Engel, M.; Small, J. P.; Steiner, M.; Freitag, M.; Green, A. A.; Hersam, M. C.; Avouris, P. *ACS Nano* **2008**, *2* (12), 2445−2452.

(7) Bahr, J. L.; Tour, J. M. *J. Mater. Chem.* **2002**, *12* (7), 1952−1958.

(8) Tu, X.; Manohar, S.; Jagota, A.; Zheng, M. *Nature* **2009**, *460* (7252), 250−253.

(9) Arnold, M. S.; Green, A. A.; Hulvat, J. F.; Stupp, S. I.; Hersam, M. C. *Nat. Nanotechnol.* **2006**, *1* (1), 60−65.

(10) Koleilat, G. I.; Levina, L.; Shukla, H.; Myrskog, S. H.; Hinds, S.; Pattantyus-Abraham, A. G.; Sargent, E. H. *ACS Nano* **2008**, *2* (5), 833−840.

(11) Yu, G.; Lieber, C. *Pure Appl. Chem.* **2010**, *82* (12), 2295.

(12) Copen Goldstein, S.; Budiu, M. NanoFabrics: spatial computing using molecular electronics. In Proceedings of 28th Annual International Symposium on Computer Architecture; 2001; pp 178−189.

(13) Heath, J. R.; Kuekes, P. J.; Snider, G. S.; Williams, R. S. *Science* **1998**, *280* (5370), 1716−1721.

(14) Hu, X. S.; Khitun, A.; Likharev, K. K.; Niemier, M. T.; Bao, M.; Wang, K. Design and defect tolerance beyond CMOS. In Proceedings of the 6th IEEE/ACM/IFIP international conference on Hardware/Software codesign and system synthesis; ACM: Atlanta, GA, 2008; pp 223−230.

(15) Rueckes, T.; Kim, K.; Joselevich, E.; Tseng, G. Y.; Cheung, C.-L.; Lieber, C. M. *Science* **2000**, *289* (5476), 94−97.

(16) Green, J. E.; Wook Choi, J.; Boukai, A.; Bunimovich, Y.; Johnston-Halperin, E.; DeIonno, E.; Luo, Y.; Sheriff, B. A.; Xu, K.; Shik Shin, Y.; Tseng, H.-R.; Stoddart, J. F.; Heath, J. R. *Nature* **2007**, *445* (7126), 414−417.

(17) Lu, W.; Lieber, C. M. *Nat. Mater.* **2007**, *6* (11), 841−850.

(18) Li, X.; Zhang, L.; Wang, X.; Shimoyama, I.; Sun, X.; Seo, W.-S.; Dai, H. *J. Am. Chem. Soc.* **2007**, *129* (16), 4890−4891.

(19) Vijayaraghavan, A.; Blatt, S.; Weissenberger, D.; Oron-Carl, M.; Hennrich, F.; Gerthsen, D.; Hahn, H.; Krupke, R. *Nano Lett.* **2007**, *7* (6), 1556−1560.

(20) Huang, Y.; Duan, X.; Wei, Q.; Lieber, C. M. *Science* **2001**, *291* (5504), 630−633.

(21) Duan, X.; Huang, Y.; Cui, Y.; Wang, J.; Lieber, C. M. *Nature* **2001**, *409* (6816), 66−69.

(22) Lu, Y.; Bangsaruntip, S.; Wang, X.; Zhang, L.; Nishi, Y.; Dai, H. *J. Am. Chem. Soc.* **2006**, *128* (11), 3518−3519.

(23) LeeM, ImJ; Lee, B. Y.; Myung, S; Kang, J; Huang, L; Kwon, Y. K.; Hong, S. *Nat. Nanotechnol.* **2006**, *1* (1), 66−71.

(24) Maune, H. T.; Han, S.-p.; Barish, R. D.; Bockrath, M.; Goddard, I. I. A.; RothemundPaul, W. K.; Winfree, E. *Nat. Nanotechnol.* **2010**, *5* (1), 61−66.

(25) Zheng, M.; Jagota, A.; Strano, M. S.; Santos, A. P.; Barone, P.; Chou, S. G.; Diner, B. A.; Dresselhaus, M. S.; Mclean, R. S.; Onoa, G. B.; Samsonidze, G. G.; Semke, E. D.; Usrey, M.; Walls, D. J. *Science* **2003**, *302* (5650), 1545−1548.

(26) Pastré, D.; Piétrement, O.; Fusil, S.; Landousy, F.; Jeusset, J.; David, M.-O.; Hamon, L.; Le Cam, E.; Zozime, A. *Biophys. J.* **2003**, *85* (4), 2507−2518.

(27) Jung, S.-Y.; Holden, M. A.; Cremer, P. S.; Collier, C. P. *ChemPhysChem* **2005**, *6* (3), 423−426.

(28) Bachilo, S. M.; Balzano, L.; Herrera, J. E.; Pompeo, F.; Resasco, D. E.; Weisman, R. B. *J. Am. Chem. Soc.* **2003**, *125* (37), 11186−11187.

(29) Chiang, I. W.; Brinson, B. E.; Huang, A. Y.; Willis, P. A.; Bronikowski, M. J.; Margrave, J. L.; Smalley, R. E.; Hauge, R. H. *J. Phys. Chem. B* **2001**, *105* (35), 8297−8301.

(30) Macfarlane, R. J.; Lee, B.; Hill, H. D.; Senesi, A. J.; Seifert, S.; Mirkin, C. A. *Proc. Natl. Acad. Sci. U.S.A.* **2009**, *106* (26), 10493−10498.

(31) Yang, S.-M.; Kim, S.-H.; Lim, J.-M.; Yi, G.-R. *J. Mater. Chem.* **2008**, *18* (19), 2177−2190.

(32) Tsai, J.; Sun, E.; Gao, Y.; Hone, J. C.; Kam, L. C. *Nano Lett.* **2008**, *8* (2), 425−430.

(33) Alivisatos, A. P.; Johnsson, K. P.; Peng, X.; Wilson, T. E.; Loweth, C. J.; Bruchez, M. P.; Schultz, P. G. *Nature* **1996**, *382* (6592), 609−611.

(34) Mirkin, C. A.; Letsinger, R. L.; Mucic, R. C.; Storhoff, J. J. *Nature* **1996**, *382* (6592), 607−609.

(35) Leunissen, M. E.; Dreyfus, R.; Cheong, F. C.; Grier, D. G.; Sha, R.; Seeman, N. C.; Chaikin, P. M. *Nat. Mater.* **2009**, *8* (7), 590−595.

(36) Sun, X.; Hyeon, Ko, S.; Zhang, C.; Ribbe, A. E.; Mao, C. *J. Am. Chem. Soc.* **2009**, *131* (37), 13248−13249.

(37) Shimizu, T; Haruyama, J; Marcano, D. C.; Kosinkin, D. V.; Tour, J. M.; Hirose, K; Suenaga, K. *Nat. Nanotechnol.* **2011**, *6* (1), 45−50.

(38) Rutherglen, C.; Jain, D.; Burke, P. *Nat Nano* **2009**, *4* (12), 811−819.

(39) Joh, D. Y.; Kinder, J.; Herman, L. H.; Ju, S.-Y.; Segal, M. A.; Johnson, J. N.; ChanGarnet, K. L.; Park, J. *Nat. Nanotechnol.* **2011**, *6* (1), 51−56.

(40) Park, C.-H.; Son, Y.-W.; Yang, L.; Cohen, M. L.; Louie, S. G. *Nano Lett.* **2008**, *8* (9), 2920−2924.

(41) Hall, A. R.; Scott, A.; Rotem, D.; Mehta, K. K.; Bayley, H.; Dekker, C. *Nat. Nanotechnol.* **2010**, *5* (12), 874−877.

(42) Guo, X.; Gorodetsky, A. A.; Hone, J.; Barton, J. K.; Nuckolls, C. *Nat. Nanotechnol.* **2008**, *3* (3), 163−167.

(43) Davis, J. J.; Morgan, D. A.; Wrathmell, C. L.; Axford, D. N.; Zhao, J.; Wang, N. *J. Mater. Chem.* **2005**, *15* (22), 2160−2174.

(44) Clarke, J.; Wu, H.-C.; Jayasinghe, L.; Patel, A.; Reid, S.; Bayley, H. *Nat. Nanotechnol.* **2009**, *4* (4), 265−270.

(45) Diehl, M. R.; Steuerman, D. W.; Tseng, H.-R.; Vignon, S. A.; Star, A.; Celestre, P. C.; Stoddart, J. F.; Heath, J. R. *ChemPhysChem* **2003**, *4* (12), 1335−1339.

(46) Lee, C. Y.; Baik, S.; Zhang, J.; Masel, R. I.; Strano, M. S. *J. Phys. Chem. B* **2006**, *110* (23), 11055−11061.